# Analysis Of Transient-MHD-Induced Magnetic Reconnection

**J.D. Callen, M.T. Beidler, C.C. Hegna, University of Wisconsin, Madison, WI**

*The Sherwood Fusion Theory Conference, Auburn, AL, April 23-25, 2018*

*Issues to be addressed:*

1) **How do ideal MHD transients induce magnetic reconnection?**

2) **Criteria for transitions to low-flow, locked-response state?**

*Outline:*

- **Motivation—ELMs, transients cause phase transitions (p 2–3).**
- **Equilibrium with flow and a small resonant 3-D field (p 4–5).**
- **Analytic theory of responses to a MHD transient (p 6–10):**
  **$B_{\rm res}$ response to transient MHD resonant magnetic perturbation (RMP),**
  **electromagnetic (EM) force induced by a temporally growing RMP,**
  **flow response to EM force that can lock flow and $B_{\rm res}$ to existing 3-D RMP,**
  **criteria for MHD transient to produce penetrated, locked-response state.**
- **Application to NIMROD results, RMP ELM suppression (p 11–14).**
- **Summary**

# ELM Precipitates[1] Bifurcation In $\delta B_\theta$ and $V_{Ct}$

[1] J.D. Callen, R. Nazikian, C. Paz-Soldan, N.M. Ferraro, M.T. Beidler, C.C. Hegna and R.J. La Haye, "Model of n = 2 RMP ELM suppression in DIII-D," report UW-CPTC 16-4, 19 December 2016, available via `https://cptc.wisc.edu` (being revised, to be published).

- **At $t \gtrsim 4705$ ms $> t_2$ in DIII-D discharge 158115 with RMPs**

  **an ELM (green bar) occurs,**

  **after which HFS $n = 2$ $\delta B_\theta$ increases abruptly* ($\lesssim$ ms)**

  **and the edge carbon flow begins* to increase.**

- **On longer time scales:**

  **the extra* $\delta B_\theta$ continues growing** up to $t_3$,**

  **carbon flow speed ($V_{Ct}$) also grows** up to $t_3$, but**

  **after 4860 ms pedestal bifurcates back to ELMing state, as applied RMPs get smaller.**

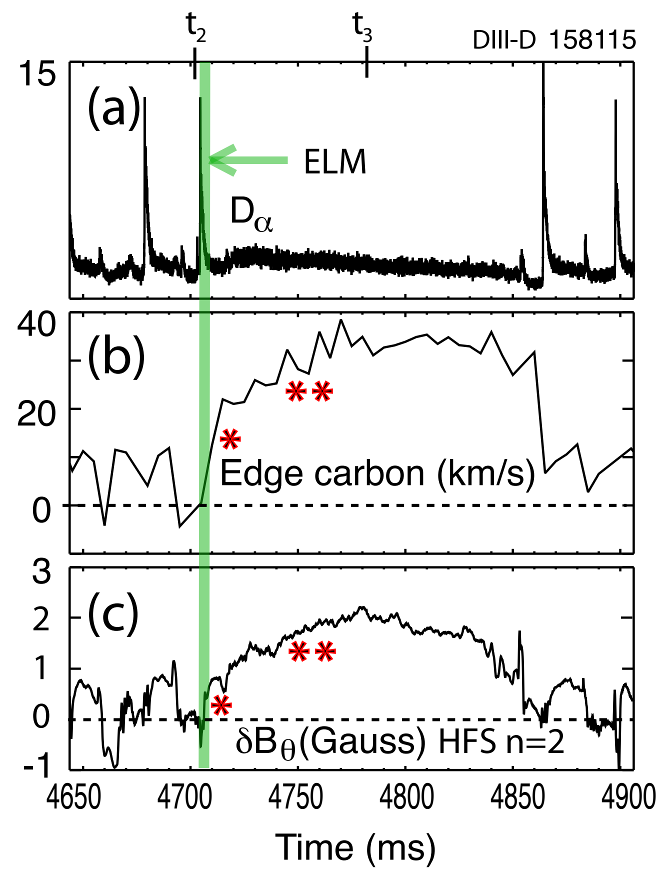


Figure 1: **Medium time scale of the bifurcation induced by the ELM at 4705 ms that occurs when applied RMPs are largest.**[1]

# NIMROD Results Are Sensitive To Size Of Transient[2]

[2] M. Beidler et al., "Nonlinear Mode Penetration Caused By Transient Magnetic Perturbations," 9:30 am talk, Wednesday, 2018 Sherwood Conference.

- **MHD transients $B_{\mathrm{ext,T}}$ are applied in NIMROD slab model**

  **for 1 ms $= 0.0069 \times 10^5 \tau_A$ ($\tau_A \equiv a/c_A \simeq 1.45 \times 10^{-6}$ s)**

  **<u>with slightly different amplitudes</u>:**

  **$B_{\mathrm{ext,T}}/B_{\mathrm{ext,0}} = 9$ (blue, solid), and**

  **$B_{\mathrm{ext,T}}/B_{\mathrm{ext,0}} = 7.75$ (red, dashed).**

- **Responses to smaller (red) transient return to initial state, but for slightly larger (blue) transient**

  **<u>resonant field at rational surface</u>**

  **<u>$B_{\mathrm{res}}$</u> increases to transient-induced reconnected/penetrated value, and**

  **<u>resonant flow frequency $\omega_{\mathrm{res}} \equiv k_y V_{\mathrm{res}}$</u> is driven to low-flow, locked-response state.**

- **Ultimate reconnection induced by MHD transient is very sensitive to its magnitude.**

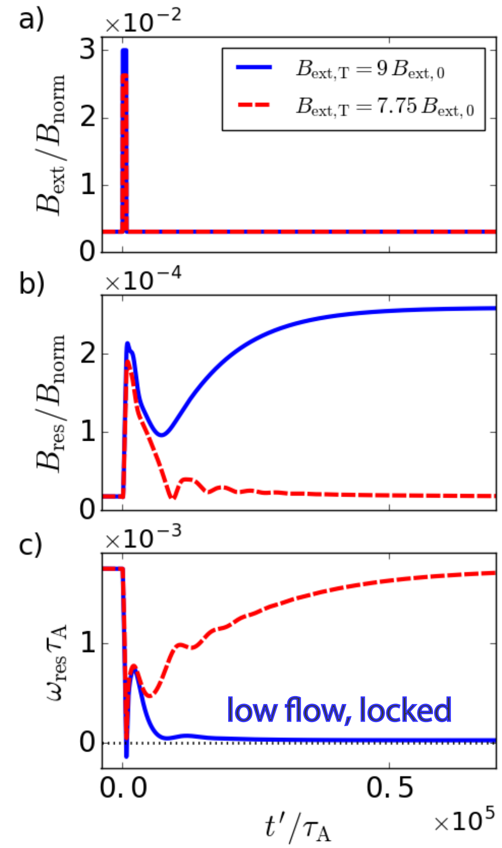


Figure 2: **Temporal evolution of responses to short resonant MHD perturbations.**

# Start From Equilibrium Magnetic Reconnection Theory[3]

- **RMP-induced equilibrium 3-D field at resonant surface is[3,4]**

$$\boxed{B_{\rm res} = \frac{(a\Delta'_{\rm ext})\,B_{\rm ext,0}}{-a\Delta'_0 + i\,\omega_{\rm res}\tau_{\rm VR}},}$$ in which equilibrium parameters in NIMROD calculations are[4]

$a\Delta'_{\rm ext} \simeq 0.54,\ B_{\rm ext,0} = 3\times10^{-4}\,{\rm T},\ a\Delta'_0 \simeq -\,2\,k_y a = -\,2\pi,\ \tau_{\rm VR} \simeq 2.104\,\tau_{\rm shA}S_{\rm sh}^{2/3}P_{\rm m} \simeq 0.0783$ s.

- **When $B_{\rm res}$ is initially in the flow-screened, high-slip state:**

for $\omega_{\rm res}\tau_{\rm VR} \simeq 123 \gg -a\Delta'_0 \simeq 2\pi$, small $B_{\rm res,0} \simeq \frac{(a\Delta'_{\rm ext})B_{\rm ext,0}}{i\,\omega_{\rm res}\tau_{\rm VR}} \simeq 1.3\times10^{-6}/i\,{\rm T}$ indicates a strongly flow-screened response $\sim$ out of phase with $B_{\rm ext,0}$, but in phase with $J_z = (i/k_y\mu_0)d^2B_{\rm ext,0}/dx^2$ that causes small electromagnetic (EM) $\hat{y}\cdot\vec{J}\times\vec{B}$ force in the singular (reconnection) layer $\delta_{\rm VR}$.

- **Resonant bi-normal ($\hat{y}$) flow $V_{\rm res}$ is determined from force balance:[3,4]**

$0 = \hat{F}_{y,{\rm EM}} + \hat{F}_{y,{\rm V}} \implies {\rm LHS}(x) \equiv 1/x - 1 + (\omega_0\tau'_{\rm VR})^2\,(x - x^2) = A_T\,(B_{\rm ext,0}/B_z, 0)^2$, in which $\omega_0 \equiv k_y V_0$ is initial flow frequency, $x \equiv \omega_{\rm res}/\omega_0$ and $A_T \equiv (a_\nu/4)(c_{\rm A}^2\tau_{\rm VR}/\nu_0)(a\Delta_{\rm VR}/|a\Delta'_0|)^2$.

- **Metastable equilibrium states occur when initial flow $V_0$ magnitude**

is large enough so[3] $|\omega_0| \equiv |k_y V_0| > 3\sqrt{3}/\tau'_{\rm VR}$ and RMP $B_{\rm ext,0}$ is in metastable region (see next viewgraph where $\omega_0 \simeq 1570\,{\rm rad/s}, \tau'_{\rm VR} \equiv \tau_{\rm VR}/|a\Delta'_0| \simeq 0.0125\,{\rm s}, \omega_0\tau'_{\rm VR} \simeq 19.5, A_T \simeq 7.4{\times}10^{10}$):

minimum $B_{\rm ext,0} \gtrsim B_{\rm ext,\,min} \simeq B_{z,0}\sqrt{2\,|\omega_0\tau'_{\rm VR}|/A_T} \simeq 2.3\times10^{-4}\,T$ and

maximum $B_{\rm ext,0} \lesssim B_{\rm ext,\,max} \simeq B_{z,0}\,|\omega_0\tau'_{\rm VR}|/(2\sqrt{A_T}\,) \simeq 3.6\times10^{-4}\,T$.

[3] See for example R. Fitzpatrick, "Bifurcated states of a rotating tokamak plasma in the presence of a static error-field," Phys. Plasmas **5**, 3325 (1998).

[4] M.T. Beidler, J.D. Callen, C.C. Hegna, and C.R. Sovinec, "Nonlinear modeling of forced magnetic reconnection in slab geometry with NIMROD," Phys. Plasmas **24**, 052508 (2017); Erratum **25**, 049901 (2018).

# Equil. Resonant Flow Is Determined From Force Balance[3,4]

- **The flow $V_y$ is determined from the force balance (FB)**

  $$\rho\,\frac{\partial V_y}{\partial t} = F_{y,EM} + F_{y,V},$$

  **in which the $\hat{y}$ direction forces are**
  **EM — $F_{y,EM} = \hat{y}\cdot\vec{J}\times\vec{B} = J_z B_x$,**
  **viscous — $F_{y,V} \simeq \rho\,\nu_0\,\partial^2 V_y/\partial x^2$.**

- **Upper figure shows integrated[2]**
  **dependences of resonant $\hat{F}_{y,EM}$ and $\hat{F}_{y,V}$ on the resonant flow frequency $\omega_{\rm res} \equiv k_y V_y(x\!=\!0)$ at rational surface.**

- **Lower figure shows equil. FB solution (curve, $B_{\rm norm} = 0.1$ T):**
  **3 solutions in shaded region**
  **— a metastable region —**
  **2 stable states (solid circles)**
  **1 unstable state (open circle).**

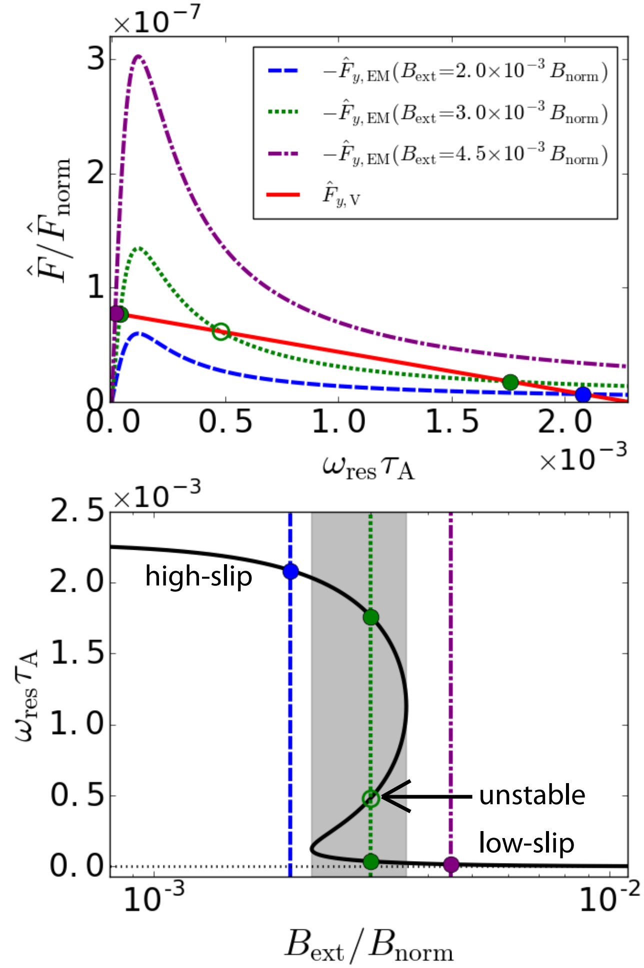


Figure 3: **EM and viscous (red) forces[2] as a function of frequency, and resonant flow frequency versus applied RMP strength.**

# How Can MHD Transients Cause Transitions To Low-Flow, Locked-Response States?

- **Hypothesis** is that MHD transients (e.g., ELMs, sawteeth) cause reconnection at rational surface ($x = 0$) and increased $\hat{F}_{y,EM}$ for a short time that can induce a locked-response state which persists.

- **Following viewgraphs develop analytic model for this hypothesis:**

  1) determine extra resonant field response $B_{\rm res}(t)$ to MHD transient $B_{\rm ext,T}$,

  2) evaluate the averaged EM force $\overline{F}_{y,EM}$ this $B_{\rm res}(t)$ induces,

  3) solve p 5 force balance equation for resultant $V_y(x,t)$ near rational surface,

  4) estimate how large $B_{\rm ext,T}$ needs to be for persistent locked-response state.

- **Final viewgraphs discuss application of analytic models to results from NIMROD calculations and key DIII-D experimental data.**

# 1) Transient MHD Perturbation Induces Reconnection

- **Equation for the radial ($\hat{x}$) component of the resonant magnetic perturbation $B_{\rm res}(t)$ at the resonant surface induced by turning on $B_{\rm ext,T}$ at $t=0$, when a $B_{\rm ext,0}$ RMP is already present, is obtained from $\hat{y}\cdot(\partial\vec{B}/\partial t = -\vec{\nabla}\times\vec{E})$ with a single-fluid resistive Ohm's law using a "constant $\psi$ regime" matched asymptotic procedure:**

$$\tau_{\rm VR}\,[\,\partial/\partial t + i\,\omega_{\rm res}(t) + 1/\tau'_{\rm VR}\,]\,B_{\rm res}(t) = (a\Delta'_{\rm ext})\,(B_{\rm ext,0} + B_{\rm ext,T}\,{\rm H}\{t\}).$$

- **Using an integrating factor, $B_{\rm res,0}$ from p 4, initial flow frequency $\omega_{\rm res}(t)\to\omega_{\rm res}(0)$, and $t/\tau'_{\rm VR}\ll 1$, the solution for $\varphi\equiv\omega_{\rm res}(0)\,t$ is**

$$B_{\rm res}(t)\;\simeq\;\frac{(a\Delta'_{\rm ext})}{i\,\omega_{\rm res}(0)\tau_{\rm VR}}\left[e^{-i\varphi}B_{\rm ext,0}+B_{\rm ext,tot}(1-e^{-i\varphi})\right],\quad \text{in which } B_{\rm ext,tot}\equiv B_{\rm ext,T}+B_{\rm ext,0}\,.$$

- **The EM force is proportional to the out-of-phase part of $B^*_{\rm res}(t)$ caused by its imaginary part, which assuming $\varphi\le 1$ and using the approximation $e^{-i\varphi}\simeq 1-i\varphi-\varphi^2/2$ yields**

$$\boxed{\mathcal{I}m\{B^{*\,\varphi\le 1}_{\rm res}\}\;\simeq\;\frac{(a\Delta'_{\rm ext})}{\omega_{\rm res}(0)\,\tau_{\rm VR}}\left[\frac{[\,\omega_{\rm res}(0)\,t]^2}{2}\,B_{\rm ext,T}+B_{\rm ext,0}\right],}\quad \text{in which in the last bracket the}$$

**$[\omega_{\rm res}(0)t]^2$ term is driven by the MHD transient and the last term is due to existing RMP.**

# 2) Out-Of-Phase $\mathcal{I}m\{B^*_{\rm res}\}$ Causes EM Force On Plasma

- **The $\hat{y}$ force balance equation on p 5 can be written as**

$$\frac{\partial V_y}{\partial t} - D_\mu \frac{\partial^2 V_y}{\partial x^2} \simeq \frac{\langle \mathcal{R}e\{J_z B^*_{\rm res}\}\rangle_{x,y}}{\rho} \equiv \frac{\overline{F}_{\rm y,EM}}{\rho}, \quad \text{in which } D_\mu \equiv \nu_0 = \frac{a^2}{\tau_\mu} \simeq 4 \text{ m}^2/\text{s}.$$

- **The average of the EM force density $F_{y,EM}$ over the thin visco-resistive layer width $\delta_{\rm VR}$ about $x = 0$ and the periodicity length $L_y \equiv 2\pi n/k_y$ is worked out as follows:**

$$\begin{aligned}
\frac{\overline{F}_{\rm y,EM}(x,t)}{\rho} &\equiv \int_{-\delta_{\rm VR}/2}^{\delta_{\rm VR}/2} \frac{dx'}{\delta_{\rm VR}} \int_{-L_y/2}^{L_y/2} \frac{dy}{L_y} \, \frac{\mathcal{R}e\{J_z(x',t)\, B^*_{\rm res}(x,t)\}}{\rho} \\
&= -\, \mathcal{I}m\{B^*_{\rm res}(t)\}\, \delta\left\{\frac{x}{\delta_{\rm VR}}\right\} \frac{1}{2\, k_y \delta_{\rm VR}\, \mu_0 \rho} \int_{-\delta_{\rm VR}/2}^{\delta_{\rm VR}/2} dx' \, \frac{d^2 B_{\rm ext,tot}(x')}{dx'^2} \\
&\simeq -\, \mathcal{I}m\{B^{*\,\varphi\le 1}_{\rm res}\}\, \mathrm{H}\{t\}\, \delta\{x\}\, \frac{(a\Delta'_{\rm ext})\, B_{\rm ext,tot}}{2\,(k_y a)\, \mu_0 \rho} \\
&= -\, \frac{V_{\rm res}(0)^2\, T_{\mathcal{E}}}{4\,(k_y a)\,[\omega_{\rm res}(0)\tau_{\rm VR}]} \left[ [\omega_{\rm res}(0)\, t]^2 + \frac{2\, B_{\rm ext,0}}{B_{\rm ext,T}} \right] \mathrm{H}\{t\}\, \delta\{x\},
\end{aligned}$$

**which uses $J_z = (i/k_y\mu_0)\, \partial^2 B_{\rm ext,tot}/\partial x^2$, $\mathcal{R}e\{iB^*_{\rm res}\} = -\,\mathcal{I}m\{B^*_{\rm res}\}\,\delta\{x/\delta_{\rm VR}\}$, $B_{\rm res}, B_{\rm ext} \propto \sin k_y y$ yields $\int_{-L_y/2}^{L_y/2} dy\ \sin^2 k_y y = L_y/2$, $\mathcal{I}m\{B^*_{\rm res}\} \simeq \mathcal{I}m\{B^{*\,\varphi\le 1}_{\rm res}\}\,\mathrm{H}\{t\}$, $\delta\{x/\delta_{\rm VR}\} = \delta_{\rm VR}\,\delta\{x\}$, $\int_{-\delta_{\rm VR}/2}^{\delta_{\rm VR}/2} dx'\, d^2 B_{\rm ext}/dx'^2 = \Delta'_{\rm ext} B_{\rm ext,tot}$, $\delta_{\rm VR} \equiv a S_{\rm sh}^{-1/3} P_{\rm m}^{1/6} \simeq 0.00745$ m is VR layer width, and**

$$T_{\mathcal{E}} \equiv \frac{(a\Delta'_{\rm ext})^2 (B_{\rm ext,T}\, B_{\rm ext,tot})/2\mu_0}{\rho_m V_{\rm res}(0)^2/2} \simeq 765,$$ **is the ratio of transient RMP to flow energy.**

# 3) Flow Responds To Transient-Induced EM Forces[2]

- **Force balance equation on p 5 is solved for $\Delta V_y \equiv V_y(x,t) - V_{\rm res}(0)$ using a local Green function**

$$G(x,t|x_0,t_0) = \frac{e^{-(x-x_0)^2/4D_\mu(t-t_0)}}{\sqrt{4\pi D_\mu(t-t_0)}}, \text{ which yields}$$

$$\boxed{\frac{\Delta V_y(x,t)}{V_{\rm res}(0)}} = \int_0^t dt_0 \int_{-\infty}^{\infty} dx_0\, G(x,t|x_0,t_0)\, \frac{\overline{F}_{\rm y,EM}(x_0,t_0)}{\rho\, V_{\rm res}(0)}$$

$$= -\frac{V_{\rm res}(0)\, T_{\mathcal{E}}}{4(k_y a)[\omega_{\rm res}(0)\tau_{\rm VR}]} \int_0^t dt_0 \frac{e^{-x^2/[4D_\mu(t-t_0)]}}{\sqrt{4\pi D_\mu(t-t_0)}} \left[ [\omega_{\rm res}(0)\, t_0]^2 + 2\,\frac{B_{\rm ext,0}}{B_{\rm ext,T}} \right]$$

$$\boxed{= -\frac{(\tau_\mu/\tau_{\rm VR})T_{\mathcal{E}}}{8\sqrt{\pi}\,(k_y a)^2} \left| \frac{\omega_{\rm res}(0)\, t}{\omega_{\rm res}(0)\,\tau_\mu} \right|^{1/2} \left[ \frac{16}{15}\,[\omega_{\rm res}(0)\, t]^2 F_{V\rm T} + 4\,\frac{B_{\rm ext,0}}{B_{\rm ext,T}} F_{V0} \right],}$$

in which the time-dependent spatial factors are

$$F_{V\rm T}[x, L_V(t)] \simeq 1 - \frac{15}{16}\sqrt{\pi}\frac{|x|}{L_V} + \frac{4}{3}\frac{x^2}{L_V^2} + \mathcal{O}\left\{\frac{|x|^3}{L_V^3}\right\},$$

$$F_{V0}[x, L_V(t)] \simeq 1 - \sqrt{\pi}\frac{|x|}{2L_V} + \frac{x^2}{4L_V^2} + \mathcal{O}\left\{\frac{|x|^3}{L_V^3}\right\}.$$

Here, at $t = 345\tau_{\rm A} \simeq 0.5$ ms $L_V(t) \equiv \sqrt{D_\mu t} \simeq 0.045$ m and $V_y(x,t) \sim$ agrees with Fig. 4 NIMROD results.[2]

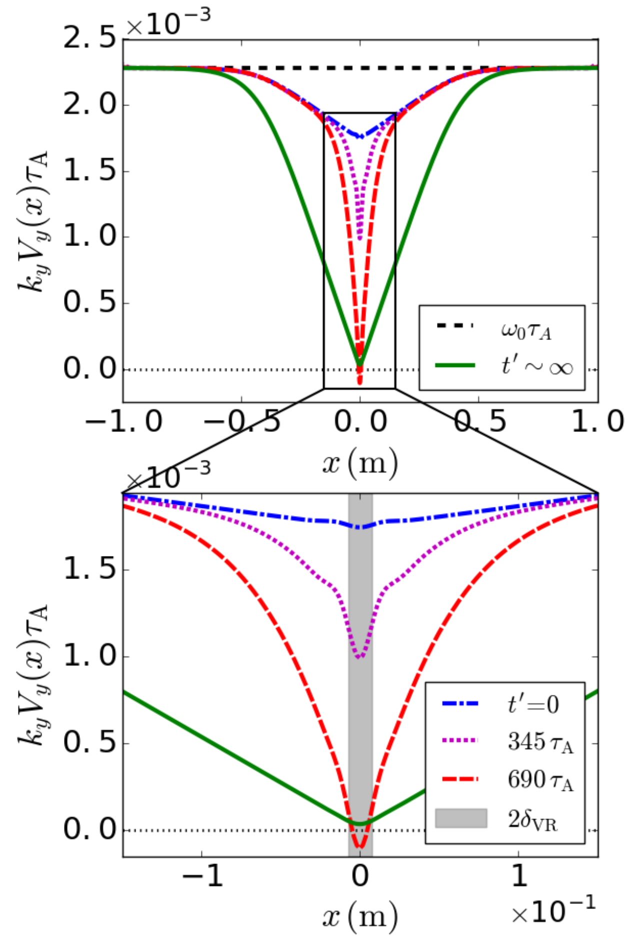


Figure 4: **Response of $V_y$ flow to EM force induced by MHD transient.**

# 4) Estimate $B_{\rm ext,T}$ Needed For Locked-Response State

- Assume the always on $B_{\rm ext,0} = 3 \times 10^{-4}$ T yields metastable states, i.e., is in the range $B_{\rm ext,\,min} < B_{\rm ext,0} < B_{\rm ext,\,max}$ on p 4 and 5.

- Hypothesize transient RMP $B_{\rm ext,T} = B_{\rm ext,tot} - B_{\rm ext,0}$ induces a persistent low-flow state if $\overline{F}_{y,EM}$ reduces flow at $x = 0$ to zero.

- Using the boxed equation on p 9, the criterion$_{\rm cr}$ in time for $\overline{F}_{y,EM}$ to force $\Delta V_y(0, t_{\rm cr})/V_{\rm res}(0) \simeq -1$ so $\omega_{\rm res}(t_{\rm cr}) \equiv k_y V_y(0, t_{\rm cr}) \to 0$ is

$$\boxed{|\omega_{\rm res}(0)\, t_{\rm cr}|^{1/2} \left[\frac{16}{15}\,[\omega_{\rm res}(0)\, t_{\rm cr}]^2 + 4\,\frac{B_{\rm ext,0}}{B_{\rm ext,T}}\right] \left(\frac{B_{\rm ext,T}\, B_{\rm ext,tot}}{B_{z,0}^2}\right) \gtrsim C_B,} \quad \text{in which}$$

$$C_B \equiv \frac{8\sqrt{\pi}\,(k_y a)^2 |\omega_{\rm res}(0)\,\tau_\mu|^{1/2}}{(\tau_\mu/\tau_{\rm VR})\,(a\Delta'_{\rm ext})^2}\,\frac{V_{\rm res}(0)^2}{c_{\rm A}^2} \simeq (2.82 \times 10^{-4})^2 \text{ and } B_{z,0} = 10 \text{ T}.$$

- At model's limit, i.e., $\varphi \equiv \omega_{\rm res}(0)\, t_{\rm cr} = 1$, this criterion predicts we need $B_{\rm ext,T}/B_{\rm ext,0} \gtrsim 6.8$, which is reasonably close to NIMROD results[2] shown in Fig. 2.

# These Reduced, Analytic Model Results Have Been Compared In Detail To NIMROD Calculations[2,4]

- **Most model predictions compare pretty well to NIMROD results:[2]**

  **upper and lower limits of $B_{\rm ext,0}$ for metastable states (p 4, 5),**

  **amount of flow-screening of $B_{\rm ext,0}$ in equilibrium for large $\omega_{\rm res}\tau_{\rm VR}$ (p 3, 4),**

  **temporal growth of $B_{\rm res}(t)$ in response[2] to applying $B_{\rm ext,T}$ (not shown here),**

  **initial space-time evolution of flow $V_y(x,t)$ in response to $B_{\rm ext,T}$ (p 9),**

  **long time temporal growth of $B_{\rm res}$ (p 3) determined from modified Rutherford equation when island width exceeds $\delta_{\rm VR}$ layer width (not shown here).**

- **However, the present models:**

  **give only rough criterion for $B_{\rm ext,T}$ needed to produce locked response (p 3, 10),**

  **and dynamics of responses after $B_{\rm ext,T}$ is turned off are not well predicted — see Beidler talk[2] at 9:30 am, Wednesday, Sherwood 2018 meeting.**

# Existence Of Metastable State Depends On Flow Frequency

- **A metastable state only occurs if there are three solutions of equilibrium force balance (see p 4, 5 and Eq. (19) in Ref. [4]):**

  $$\mathrm{LHS}(x) = A_T\,(B_{\mathrm{ext},0}/B_{z,0})^2,$$
  $$x \equiv \omega_{\mathrm{res}}/\omega_0,\; A_T \simeq 7.4\times 10^{10}.$$

- **Metastable state occurs if**

  $$\boxed{|\omega_0 \tau'_{\mathrm{VR}}| > 3\sqrt{3} \simeq 5.2.}$$

- **Without metastable states states, bifurcations cannot occur — because responses are continuous in $x$.**

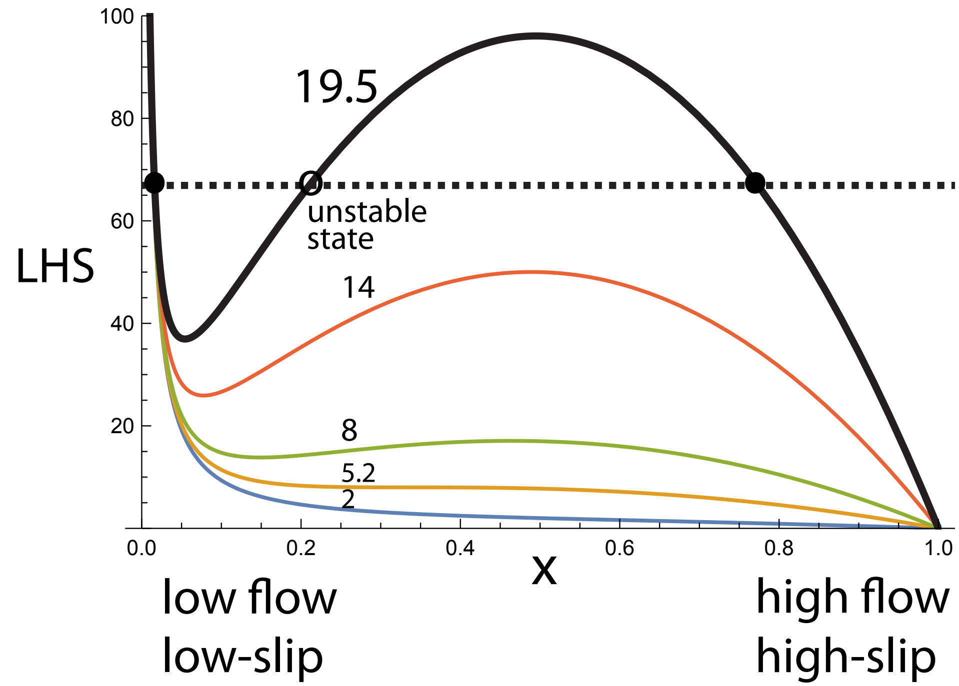


Figure 5: **Solutions of equilibrium force balance for specific values of $\omega_0\tau'_{\mathrm{VR}}$ as a function of $x \equiv \omega_{\mathrm{res}}/\omega_0$. Black curve in Figure 3 has $\omega_0\tau'_{\mathrm{VR}} = 19.5$, $A_T(B_{\mathrm{ext},0}/B_{z,0})^2 \simeq 67$, and here is inverted, rotated clockwise by 90°.**

# RMP ELM Suppression Is Not Obtained At Low Flow

- **This is observed a lot. Recent DIII-D data shown below indicates a minimum carbon flow is needed to achieve RMP ELM suppression.**

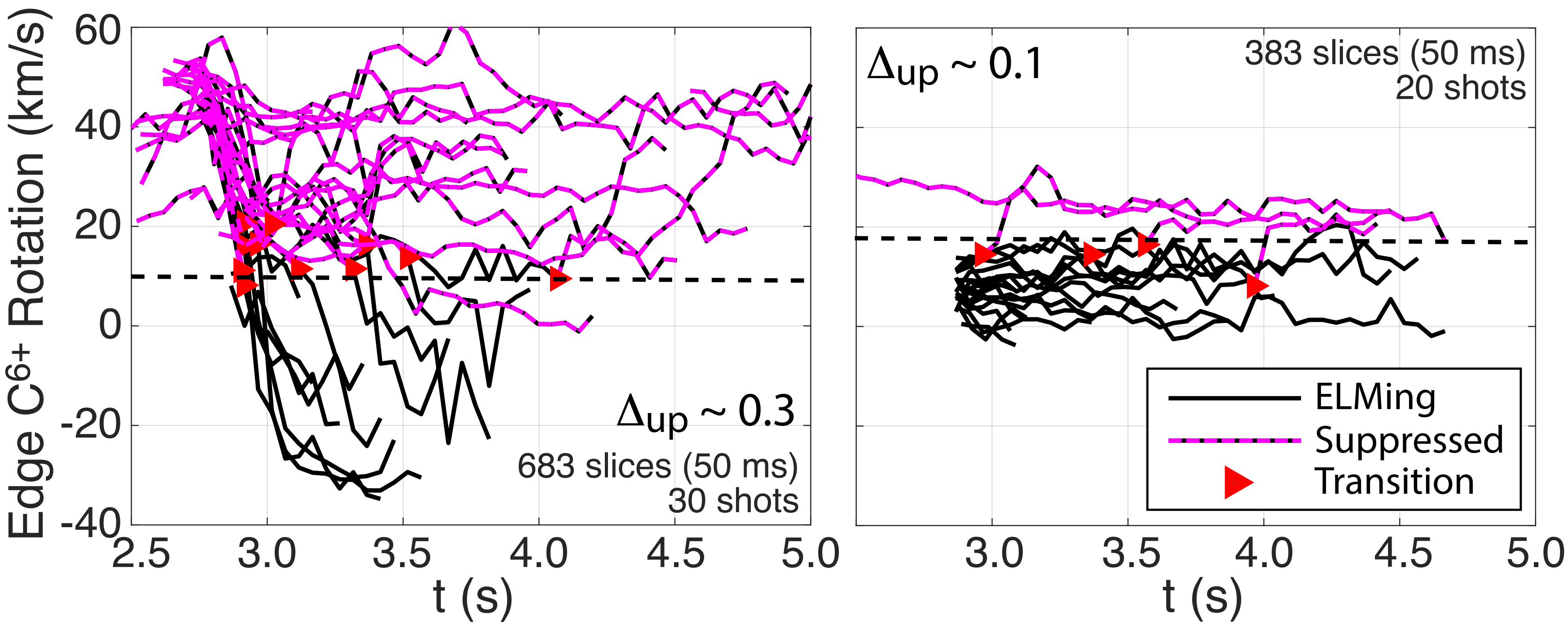


Figure 6: **Recent $n = 3$ RMP data from DIII-D shows as carbon edge toroidal flow drops below $\sim$ 10 km/s for upper triangularity of 0.3, or $\sim$ 18 km/s for upper triangularity of 0.1, RMP ELM suppression is lost. Courtesy of C. Paz-Soldan.**

# Metastable State Accessibility May Explain DIII-D Results

- **Analysis of equilibrium force balance equations shown on p 5, 12 indicates metastable state only occurs if $\omega_0\tau'_{\rm VR}$ is large enough:**
  **from idealized theory[3,4] need $|\omega_0\tau'_{\rm VR}| > 3\sqrt{3} \simeq 5.2$, or maybe more robustly, from requirement of $B_{\rm ext,max} \gtrsim B_{\rm ext,min}$ on p 4, 5 and Fig. 5 need $|\omega_0\tau'_{\rm VR}| \gtrsim 8$; here, $\omega_0 \equiv nV_y(0{,}0)/R_0$ in which $V_y(0{,}0) \simeq E_\rho/B_{\rm pol}$ at $q = m/n$ while ELMing.**

- **The relative reconnection layer time here is ($\tau'_{\rm VR} \sim 10^{-3}$ s)**

$$\tau'_{\rm VR} \equiv \frac{\tau_{\rm VR}}{|\rho_0\Delta'_0|} = \frac{2.104\,\tau_{\rm shA} S_{\rm sh}^{2/3} P_{\rm m}^{1/6}}{2\,m} \propto \frac{\rho_0^{4/3} L_{\rm sh}^{1/3}\, T_e\, n_i^{1/6} P_{\rm m}^{1/6}}{m^{4/3} B_{z,0}^{1/3} Z_{\rm eff}^{2/3}} \sim \frac{T_e}{m^{4/3} B_{z,0}^{1/3} Z_{\rm eff}^{2/3}}.$$

- **For $n = 2$ parameters[2] in DIII-D discharge 158115, corrected for $n = 3$ in Fig. 6 and assuming carbon flow is dominated by $E_\rho/B_{\rm pol}$, theoretical$^{\rm th}$ carbon toroidal flow needed for ELM suppression is**

  **$V_{\rm Ct}^{\rm th} = R\omega_0/n \gtrsim (5.2\text{–}8)R/\tau'_{\rm VR} \simeq 13\text{–}20$ km/s versus $V_{\rm Ct}^{\rm exp} \gtrsim 10\text{–}18$ km/s (Fig. 6) and predicted flow speed is smaller for higher triangularity with its higher $T_e$.**

- **Thus, minimum flow criterion for metastable state to exist roughly agrees with RMP ELM suppression conditions in DIII-D (Fig. 6) — to be tested against more DIII-D data (C. Paz-Soldan).**

# Summary

- **Small MHD transients (ELMs, sawteeth) in flowing tokamak plasmas with existing RMPs that produce metastable states can precipitate transitions into low-flow, locked-response states (p 2, 3).**

- **Quasilinear analytic models have been developed for the effects MHD transients induce (p 11):**

  **temporal increase in magnetic reconnection and hence of $B_{\rm res}(t)$ (p 7),**
  **resultant temporal evolution of the average EM force density $\overline{F}_{y,EM}$ (p 8),**
  **abrupt, localized decrease of $V_y(x,t)$ flow near the rational surface (p 9), and**
  **locked-response state if transient $B_{\rm ext,T}$ size and duration are sufficient (p 10).**

- **This quasilinear theory provides reduced models for describing**

  **NIMROD calculations of effects — Beidler talk[2] 9:30 am Wed., Sherwood 2018,**
  **RMP ELM suppression in DIII-D — why it doesn't occur at low flow (p 12–14).**